Plant Stress 12 (2024) 100489

Contents lists available at ScienceDirect

Plant Stress

journal homepage: www.sciencedirect.com/journal/plant-stress

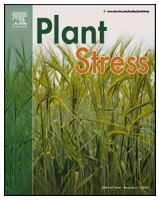

Genome-wide characterization of the glutathione *S*-transferase gene family in *Phaseolus vulgaris* reveals insight into the roles of their members in responses to multiple abiotic stresses☆

Touhidur Rahman Anik [a], Ha Duc Chu [b], Md. Shahabuddin Ahmed [c], Chien Van Ha [a], Sunil S. Gangurde [d], Md. Arifur Rahman Khan [a,e], Thao Duc Le [f], Dung Tien Le [g], Mostafa Abdelrahman [a], Lam-Son Phan Tran [a,*]

[a] *Department of Plant and Soil Science, Institute of Genomics for Crop Abiotic Stress Tolerance, Texas Tech University, Lubbock, TX 79409, USA*
[b] *Faculty of Agricultural Technology, University of Engineering and Technology, Vietnam National University Hanoi, Xuan Thuy Road, Cau Giay District, Hanoi City, 122300, Viet Nam*
[c] *Department of Biotechnology, Bangladesh Agricultural University, Mymensingh 2202, Bangladesh*
[d] *International Crops Research Institute for the Semi-Arid Tropics, Hyderabad 502324, India*
[e] *Department of Agronomy, Bangabandhu Sheikh Mujibur Rahman Agricultural University, Gazipur 1706, Bangladesh*
[f] *Agricultural Genetics Institute, Pham Van Dong Street, North Tu Liem District, Hanoi City, 122300, Viet Nam*
[g] *VK Tech Research Center, Nguyen Tat Thanh University, 298-300A Nguyen Tat Thanh Street, District 4, Ho Chi Minh City, Viet Nam*

A R T I C L E I N F O

Keywords:
Drought and salinity
Glutathione *S*-transferases
Gene expression analysis
Phaseolus vulgaris
Transcriptome data

A B S T R A C T

Glutathione *S*-transferases (GSTs) are a class of multifunctional enzymatic antioxidants that play a significant role in several aspects of plant physiology, including growth, development, and cellular protection from biotic and abiotic stressors. A total of 59 *GST* genes were found in *Phaseolus vulgaris* genome, which were categorized into 11 distinct classes according to their evolutionary connection and the existence of conserved structural domains and motifs. Gene duplication analysis revealed that the evolution of the members of the *GST* gene family in *P. vulgaris* was driven by both segmental and tandem duplication events. Analysis of the expression profiles of identified *PvGST* genes using the available transcriptome data demonstrated notable expression patterns and organ specificity of many genes throughout several developmental stages and under drought or salinity. Subsequent RT-qPCR analysis of several drought-responsive or salinity-responsive candidate genes showed that *PvGSTF4* was up-regulated solely by drought, *PvGSTU11* was up-regulated only by salinity, and *PvGSTU3, PvGSTU12, PvGSTU13, PvGSTU14, PvGSTU16, PvGSTT1*, and *PvGSTZ2* were up-regulated by both salt and drought. The up-regulated *PvGSTs* under drought and/or salinity might enable *P. vulgaris* to adapt to stressful environments. These candidate genes could be explored in genetic engineering programs for development of stress-tolerant *P. vulgaris* varieties.

Introduction

Continually facing with a barrage of environmental stresses like drought and salinity, plants have developed intricate detoxification mechanisms to counteract the harmful effects of stress-induced accumulation of reactive oxygen species (ROS) that cause oxidative damage. Among these protective systems, glutathione *S*-transferases (GSTs, EC 2.5.1.1.8) function downstream of cytochrome P450 to maintain key metabolic processes of ROS detoxification and redox buffering (Lallement et al., 2014). Moreover, GSTs play a pivotal role in combating oxidative stress by detoxifying peroxidized lipids, and thus contribute to the preservation of membrane integrity during stress conditions (Estévez and Hernández, 2020). In essence, through the versatile functions of enzymes like GSTs, plants are equipped to deal with a diverse array of environmental challenges, ensuring their survival and the health of ecosystems at large (Kumar and Trivedi, 2018).

Common bean (*Phaseolus vulgaris*) is an important dietary staple for humans. Its seeds are considered as a significant component of balanced

☆ This article is part of a special issue entitled: "Omics-assisted crop improvement under abiotic stress conditions" published at the journal Plant Stress.

* Corresponding author.
E-mail address: son.tran@ttu.edu (L.-S.P. Tran).

https://doi.org/10.1016/j.stress.2024.100489
Received 18 December 2023; Received in revised form 24 April 2024; Accepted 14 May 2024
Available online 18 May 2024

diets, mostly due to their substantial nutritional content characterized by high protein levels and low-fat content (Yang et al., 2018). Additionally, common beans are rich in carbohydrates, vitamins, phytate, lectins, soluble fiber, and phenolics, which further contribute to their recognized importance (Alcázar-Valle et al., 2020; Yang et al., 2018). Despite their economic and nutrient importance in many countries, especially in Latin America, common beans have not attracted strong interests from research community compared with other legumes like soybean (*Glycine max*) and chickpea (*Cicer arietinum*). Common beans are morphologically and genetically highly diverse due to their individual domestication from Mesoamerican and Andean gene pools (Kwak and Gepts, 2009). Additionally, common bean genome size is much smaller and less complex compared with other beans (McConnell et al., 2010). All these characteristics make common beans a suitable model crop for comparative genomics research in legumes.

Being domesticated from its wild counterparts, which occupy a very limited ecological niche, common bean encounters an array of biotic and abiotic stressors throughout its broad range of agroecological environments (Arteaga et al., 2020; Burbano-Erazo et al., 2021; Sofi et al., 2021). Particularly, abiotic stresses like drought and salinity substantially affect the production and quality of this economically important crop (Arteaga et al., 2020; Burbano-Erazo et al., 2021; Sofi et al., 2021). The availability of detailed genome sequence information of common bean (Schmutz et al. 2014) is useful for the investigation of the functions of stress-responsive genes like *GST*s. Prior studies have shown that the overexpression of different *GST* members can enhance tolerance of transgenic plants to various abiotic stresses. For example, ectopic expression of the rice (*Oryza sativa*) *OsGSTU4* and *OsGSTU30* increased tolerance of transgenic *Arabidopsis thaliana* plants to salt and oxidative stresses (Sharma et al., 2014) and drought and heavy metal stresses (Srivastava et al., 2019), respectively, while overexpression of *AtGSTU19* increased tolerance of transgenic *Arabidopsis* plants to drought and oxidative stresses (Xu et al., 2016). Similarly, ectopic expression of *A. thaliana AtGSTF11* increased tolerance of transgenic tobacco (*Nicotiana tabacum*) plants to cold and salt stress (Kuluev et al., 2022), while that of grape (*Vitis vinifera*) *VvGSTF13* improved drought, salt, and oxidative stress tolerance of transgenic *A. thaliana* plants (Xu et al., 2018). Likewise, overexpression of *OsDHAR1* increased salt tolerance of transgenic *O. sativa* plants (Kim et al., 2022), whereas ectopic expression of *OsGSTL1* enhanced tolerance of transgenic *A. thaliana* against multiple stresses, including heavy metal, salinity, cold, and osmotic stresses (Kumar et al., 2013).

To date, genome-wide analyses of the *GST* family have been performed in a large number of higher plant species, including *A. thaliana* (Sappl et al., 2009; Wagner et al., 2002), rice (Jain et al., 2010), wheat (*Triticum aestivum*) (Hao et al., 2021; Wang et al., 2019), barley (*Hordeum vulgare*) (Rezaei et al., 2013), cottons (*Gossypium raimondii* and *G. arboreum*) (Dong et al., 2016), barrel clover (*Medicago truncatula*) (Han et al., 2018), mung bean (*Vigna radiata*) (Vaish et al., 2018), chickpea (Ghangal et al., 2020), soybean (Hasan et al., 2020), apple (*Malus domestica*) (Fang et al., 2020), and foxtail millet (*Setaria italica*) (Wang et al., 2023), highlighting the large interest of the research community in elucidating the functions of the members of this gene family in plant development and stress adaptation. Thus, in this study, we aimed to systematically identify, characterize, and provide a comprehensive overview about the expression patterns of the *GST* family members in *P. vulgaris* in different organs and under drought and salinity. Findings of this study will serve as a crucial foundation for identifying stress-responsive *GST* genes in common bean and advancing development of improved stress-tolerant common bean varieties.

Materials and methods

Bioinformatic analyses

The current study used the GSTs from *Arabidopsis* (Sappl et al., 2009), rice (Jain et al., 2010), soybean (Hasan et al., 2020), and barrel clover (Hasan et al., 2021) to identify putative GST members in *P. vulgaris*. Annotated *Arabidopsis,* rice, soybean, and barrel clover GST protein sequences were obtained from the Ensembl Plants database (http://plants.ensembl.org/index.html). BLASTp searches were performed against the whole common bean protein sequences obtained from the Ensembl Plants database with a 10^{-10} cut-off e-value and a bit-score $\geq$ 100 (Islam et al. 2021). After filtering out duplicate sequences, we searched for transmembrane domains using the Pfam (http://pfam.xfam.org) (Mistry et al., 2021) and NCBI conserved domain database (NCBI CDD, https://www.ncbi.nlm.nih.gov/Structure/cdd/wrpsb.cgi) (Lu et al., 2020). The protein sequences possessing the GST-related domain were compiled, and all the candidate GST proteins were named using the previously proposed approach, with the prefix 'Pv' for *P. vulgaris*, followed by a class identifier (*e.g.*, PvGSTU, PvGSTF, PvGSTT, PvGSTZ, PvGSTL, PvTCHQD, PvDHAR, PvEF1BG, PvMGST, PvGHR, and PvGSTM represents tau, phi, theta, zeta, lambda, TCHQD, DHAR, EF1Bγ, mPEGS2, GHR, and metaxin class, respectively) and a sequential number (*e.g.*, PvGSTU1) for each protein (Dixon et al., 2002; Hasan et al., 2021). The ProtParam software (https://web.expasy.org/protparam) was employed to estimate the length, molecular weight (mW), instability index (II), isoelectric point (pI), aliphatic index (AI), and grand average of hydropathicity (GRAVY) of identified common bean GST proteins (Gasteiger et al. 2005).

The chromosomal distribution of the *PvGST* genes in *P. vulgaris* genome was explored using the Ensembl Plants BioMart (Contreras-Moreira et al., 2022), and their location on the *P. vulgaris* genome was then illustrated using the TBtools software (Chen et al., 2020). To examine the duplication events among the putative *PvGST* genes, an identity matrix was developed based on their nucleotide sequences, applying a threshold of greater than 70 % identity. Duplication events were classified as segmental or tandem, depending on whether the duplicated *PvGST* genes were located on different chromosomes or within the same chromosome in a region spanning 20 Kb, respectively. The non-synonymous substitution rate, denoted by Ka, the synonymous substitution rate, denoted by Ks, and the ratio of Ka to Ks were calculated using the TBtools. The TBtools was also used to estimate the synteny links between the *GST* genes of *P. vulgaris* and those of many other plant species, including *Arabidopsis*, rice, mung bean, soybean, chickpea, and barrel clover.

Full-length PvGST protein sequences from common bean, *Arabidopsis*, rice, soybean, mung bean, barrel clover, and chickpea were used to generate a phylogenetic tree using the maximum likelihood algorithm (Islam et al., 2021, 2017) with the aid of MEGA11 software (Tamura et al., 2021). A total of 1000 bootstrap values were utilized in the process. TBtools was used to determine the exon-intron distribution within each of the *PvGST* genes by aligning the coding sequences and their associated genomic sequences. Subcellular localizations of the PvGST proteins were predicted using Cello (http://cello.life.nctu.edu.tw) (Yu et al., 2006).

The GST domains obtained from the NCBI CDD database were used in the structural analysis and visualized using the TBtools. Conserved motifs in the PvGST protein sequences were predicted by exploring the Multiple Expectation Maximization for Motif Elicitation (MEME, http://meme-suite.org/tools/meme) tool (Bailey et al., 2015). Only 10 motifs, with the breadth of each motif limited to 10 - 50 amino acid residues, were shown using TBtools. The Ensembl Plants BioMart database was employed to retrieve the 2 Kb promoter sequences of 59 *PvGST*s from upstream region of the start codon, which were then uploaded to PlantCARE (https://bioinformatics.psb.ugent.be/webtools/plantcare/html/) (Lescot et al., 2002) in order to locate the *cis*-regulatory elements (CREs).

We used the PvGEA: Common Beam Gene Expression Atlas and Network Analysis (https://www.zhaolab.org/PvGEA/) database to obtain the gene expression datasets of *P. vulgaris* under normal growth conditions across six organs at several developmental stages, including

fully developed 2nd trifoliate leaves (leaf), stem internodes atop the cotyledon collected at the 2nd trifoliate stage (stem), shoot tips with apical meristem collected at the 2nd trifoliate stage (shoot), flower collected before floral emergence (flower), pods (excluding seeds) collected at one to four days after floral senescence [pod (young)], pods (excluding seeds) around 9 cm long [pod (9 cm)], pods (excluding seeds) between 10 and 11 cm [pod (10 cm)], pods (excluding seeds) between 12 and 13 cm [pod (12 cm)]; seeds at heart stage weighted around 7 mg [seed (7 mg)], stage one seeds weighted around 50 mg [seed (50 mg)], stage two seeds weighted around 50 mg [seed (50 mg)], root tips collected at 2nd trifoliate stage (root tip), whole root with root tips collected at 2nd trifoliate stage (root) (O'Rourke et al., 2014). To explore the expression profiles of the *PvGST* genes in common bean under drought and salinity, the following RNA-sequencing datasets were used: drought [GSE123381, leaves of common bean plants subjected to progressive drought imposed by suspending irrigation for 14 days at the V4 stage (45-days after planting)] (Gregorio Jorge et al., 2020), salinity [GSE156113, leaves and roots from two contrasting common bean plants subjected to gradual salinity at early seedling stage (14-day-old seedlings)] (Niron et al., 2020). The "gradual step acclimation" approach was employed by providing salt (NaCl) to hydroponic nutrient solution at 50 mM on the 1st day, 100 mM on the 2nd day, and 125 mM on days three to five. All the expression data were further visualized using the R Studio 1.4.1717 (http://www.rstudio.com/). A gene was considered up- or down-regulated in drought treatment if its $\log_2$ (fold change) ≥ 1.00 or ≤ -1.00 ($p \leq 0.05$) (Gregorio Jorge et al., 2020), whereas a gene was considered up- or down-regulated in saline condition if its $\log_2$ (fold change) ≥ 1.00 or ≤ -1.00 ($q \leq 0.01$) (Niron et al., 2020). In the heatmap, the *PvGST* genes were divided into separate clusters depending on their expression levels/changes using Euclidean distance-based hierarchical clustering method.

Plant materials and stress treatment

Healthy common bean (pinto bean) seeds (15 seeds per pot) were directly sown in 1-gallon plastic pots containing 1 Kg BM-7 professional potting mix (https://www.berger.ca/en/horticultural-products/bm7-bark/). Ten equally grown seedlings were kept in each pot. The experiment was carried out in a growth chamber with the following conditions: temperature: 30 °C, photon flux density: 200 μmol m^{-2} s^{-1}, day/night ratio: 14-h light/10-h dark, and relative humidity: 50 %. The seedlings were grown till V2 stage (2nd trifoliate). After that, plants were separated into three groups (each group containing 10 pots): 1st group was subjected to water-withholding-induced drought stress, 2nd group was subjected to 200-mM NaCl-induced salinity stress, and 3rd group were kept growing under normal irrigation system (0 mM NaCl). For salinity stress treatment, two pots were kept in a tray and 3 L of 200-mM NaCl solution were provided at 3-day intervals. In both stress conditions samples were collected at five and seven days after stress. The 2nd trifoliate leaves from the top were chosen for physiological, biochemical, and gene expression analyses. For biochemical and reverse transcription-quantitative polymerase chain reaction (RT-qPCR) analyses, collected samples were immediately frozen in liquid nitrogen and then stored at −80 °C.

Physiological and biochemical analyses

Leaf relative water content (RWC) and electrolyte leakage (EL%) were determined following the methods of Nishiyama et al. (2011) and Emamverdian et al. (2023) respectively. Histochemical detection of hydrogen peroxide (H_2O_2) in common bean leaves was performed using 3,3′-diaminobenzidine (DAB) staining following the method described by Mostofa and Fujita (2013). For quantifying the activities of GSTs, leaf samples (0.3 g) were crushed in 1 mL of 50 mM ice-cold potassium--phosphate buffer (pH 7.0), containing 1 mM EDTA. The homogenized plant material was centrifugated at 12,000 × rpm (revolutions per minute) for 12 min, and the supernatant was collected for estimating GST activity using the Glutathione *S*-Transferase Assay Kit (Cayman Chemical, Ann Arbor, MI, United States; catalog number: 703,302) according to the manufacturer's instructions. The same sample extract was also used to measure the content of H_2O_2 using the Amplex Red Hydrogen Peroxide/Peroxidase Assay Kit (Invitrogen, Eugene, OR, United States; catalog number: A22188) according to the manufacturer's instructions.

RNA extraction and RT-qPCR analysis

The total RNA was extracted from collected leaf samples using the RNeasy Plant Mini Kit (QIAGEN, Hilden, Germany; catalog number: 74,903 and 74,904) with the aid of QUIcube Connect (QIAGEN, Hilden, Germany) nucleic acid extraction machine according to the manufacturer's instructions. Genomic DNA (gDNA) was removed from the extracted RNA using RNase-free DNase Set (QIAGEN, Hilden, Germany; catalog number: 79,254) according to the manufacturer's instructions. One μg of gDNA-free total RNA was utilized for the synthesis of complementary DNA (cDNA) using QuantiTect Reverse Transcription Kit (QIAGEN, Hilden, Germany; catalog number: 79,254) for a RT-qPCR analysis. The expression levels of selected *PvGST* genes (Table S1) were analyzed by RT-qPCR using SsoAdvanced Universal SYBR Green Supermix (Bio-Rad, Hercules, CA, United States; catalog number: 1,725,274) following manufacturer's instructions. Bio-Rad CFX96 Real-Time System (Bio-Rad, Hercules, CA, United States) was used to carry out the RT-qPCR. *PvTubulin beta8* gene was used as housekeeping gene (Borges et al., 2012). The data of RT-qPCR was analyzed using $2^{-\Delta Cq}$ method. A gene was defined as up-regulated when its expression level increased by ≥ 2.00 fold with a *p*-value ≤ 0.05.

Statistical analysis

The data were presented as the mean values together with their corresponding standard deviation, which were calculated based on five biological replicates for each treatment in case of biochemical and physiological analyses, and three biological replicates for each treatment in case of RT-qPCR analysis. The data were subjected to a statistical analysis using a one-way analysis of variance (ANOVA) followed by a least significant difference test to compare the means of the different treatments. The significance level was set at $p < 0.05$. The statistical analyses were conducted using the Statistix 10.0 software (https://www.statistix.com/).

Results

Identification and annotation of the PvGST genes in P. vulgaris

A comprehensive set of 59 PvGST proteins were identified in *P. vulgaris* which can be classified in 11 classes (Table S2). Twenty-seven PvGST proteins were classified under the tau class. The phi class had 12 members and lambda class consisted of four members, while the theta, zeta, TCHQD, DHAR, EF1Bγ, mPEGS2, GHR, and metaxin classes each comprised two PvGST members (Table S2). The protein sequences under consideration were derived from a total of 59 *PvGST* genes. The lengths of the coding sequences ranged from 1263 (*PvEF1BG1*) to 420 bp (*PvGSTU27*) (Table S3). Additionally, the amino acid lengths of the proteins ranged from 420 (PvEF1BG1) to 139 residues (PvGSTU27) (Table S3). According to the mW data, PvEF1BG2 exhibited the highest protein size of 47.99 kDa, while PvGSTU27 displayed the smallest protein size of 15.76 kDa (Table S3). Furthermore, an analysis was conducted on additional parameters including the II (with a range spanning from 23.26 to 54.77), pI (ranging from 5.03 to 9.61), AI (ranging from 75.27 to 105.76), and GRAVY (ranging from −0.514 to 0.01) (Table S3). The cytoplasm was shown to be the primary subcellular localization for the bulk of the PvGST proteins, followed by the mitochondria,

chloroplast, endoplasmic reticulum, extracellular space, and nucleus.

Chromosomal distribution and gene duplication event of the PvGST genes

The studied *PvGST* genes were mapped on 11 chromosomes of *P. vulgaris* genome. The highest number of *PvGST*s, 11 genes, was mapped on chromosome 7 followed by seven genes on each of chromosomes 5 and 6, six on each of chromosomes 2, 8, and 9, five on each of chromosomes 1 and 3, four on chromosome 10, and one gene on each of chromosomes 4 and 11 (Fig. 1). The *PvGST* family members exhibited a total of 12 segmental duplication events across 10 different chromosomes (Fig. 1, Table S4). Additionally, eight tandem duplication events were also observed in the *PvGST* gene family (Fig. 1, Table S4). To facilitate further examination into the selection pressure exerted on the duplicated genes, the Ka/Ks value was computed. The Ka/Ks values for all duplicated genes were below 1, ranging from 0.10 to 0.74. These results suggested that purifying selection pressure has played a significant role in shaping the evolutionary process of these gene pairs. Furthermore, the estimated divergence period of the duplicated gene pairs exhibited a range from 209.61 to 2.17 million years ago (Table S4).

Structure of the PvGST genes

The gene structure of the *PvGST* family members exhibited a substantial amount of diversity. While there was considerable structural heterogeneity among distinct classes of *PvGST*s, genes within the same class had comparable gene architectures (Fig. 2). All members of the tau class exhibited singular introns and were classified as phase 0 introns. The members of the phi class exhibited the presence of one to two introns, which were classified as phases 0 and 1 introns. The lambda class members were shown to possess a total of eight to nine introns, distributed among phases 0, 1, and 2. All members of the theta class possessed a total of six introns, which were categorized into phases 0, 1, and 2. The members of the zeta class were found to possess a total of eight to nine introns, which were classified as either phase 0 or phase 1. All members of the DHAR class possessed a total of five introns, belonging to all three phases (0, 1, and 2). All members of the mPEGS2 group were found to possess a total of five introns, which were classified as either the 1 or 2 phases. All members of the TCHQD possessed a single intron that belonged to phase 2. The members of the EF1Bγ class were found to possess a total of four to five introns, which were classified as either phase 0 or phase 1. Members of the GHR class exhibited either two or four introns and were classified as phase 0 or 2. Lastly, members of the metaxin class had five introns and were categorized into either phase 1 or 2.

Conserved domain and motif analyses of the PvGST proteins

Analysis of the domain architecture revealed that 33 of the PvGST proteins contained both N-terminal and C-terminal GST domains, while 21 PvGST contained only N-terminal GST domain and five PvGST contained only C-terminal GST domain (Figure S1). PvEF1BG1 and PvEF1BG2 were found to contain specific C-terminal EF1Bγ domain in addition to N-terminal GST domain (Figure S1). PvMGST1 and PvMGST2 proteins contained distinct C-terminal mPEGS2 domain along N-terminal GST domain, while PvGSTM1 and PvGSTM2 proteins possessed C-terminal metaxin and N-terminal GST domains (Figure S1).

In this study, a total of 10 motifs that exhibit a high degree of conservation and possess a length exceeding ten amino acids were successfully found on PvGST proteins (Figure S2 and Table S5). No conserved motif was found for PvGSTM1 and PvGSTM2 proteins. A total of 51 PvGST proteins, excluding PvGHR1, PvGHR2, PvGSTU24, PvGSTU27, PvMGST2, PvGSTF1, PvGSTM1, and PvGSTM2, contained motif 1. Motif 2 was exclusive for the tau, lambda, and zeta class PvGST proteins. Motif 3 was observed to be ubiquitously present in most members of the PvGST family except for PvGSTU17, PvGSTM1, and PvGSTM2. Motif 4 was unique to tau, phi, DHAR, zeta, and TCHQD PvGST proteins. Motif 5 was only found in PvGSTs of the tau and lambda classes, whereas motif 10 was found only in the tau PvGSTs. The EF1Bγ and phi classes of PvGST proteins shared motif 6, but only phi class PvGSTs possessed motif 7. Motif 8 appeared in the majority of PvGST proteins, while motif 9 was unique to the GHR and lambda class PvGST proteins.

Phylogenetic and synteny analyses of the PvGST proteins

To infer the evolutionary relatedness of PvGST family proteins, a phylogenetic tree was created using the maximum likelihood method. This involved a comprehensive set of 442 GST protein sequences obtained from several plant species, including *Arabidopsis*, rice, soybean, mung bean, barrel clover, and chickpea. The GST proteins were classified into 12 distinct clusters, as depicted in Figure S3. Despite the inclusion of GST proteins from both monocot and dicot plant species in the construction of the phylogenetic tree, it was observed that the GST proteins from both monocots and dicots were clustered together. Another interesting observation is that all the clusters were exclusively composed of monophyletic groups. Moreover, the clustering analysis provided strong support for the domain-based classification of the PvGST proteins. It was evident from the phylogenetic tree that the tau-class GSTs exhibit the highest magnitude in terms of member size among all GST classes, followed by the phi and lambda classes. The members of the other GST classes were variable in size among the species.

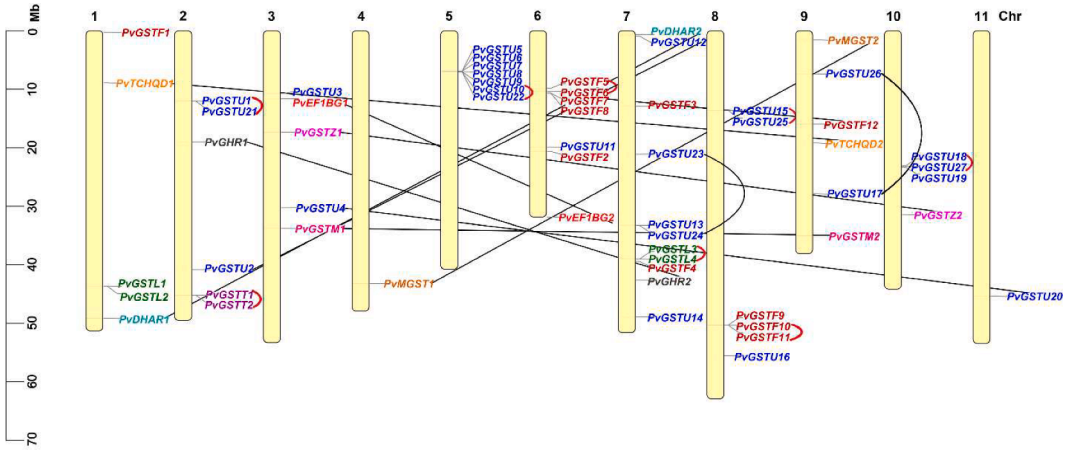

Fig. 1. Schematic diagram of chromosomal location and duplication events of 59 *PvGST* genes. The vertical scale (Mb) on the side indicates chromosome (Chr) size and gene position on the chromosomes. Black and red lines connected the segmental and tandem duplicated gene pairs, respectively.

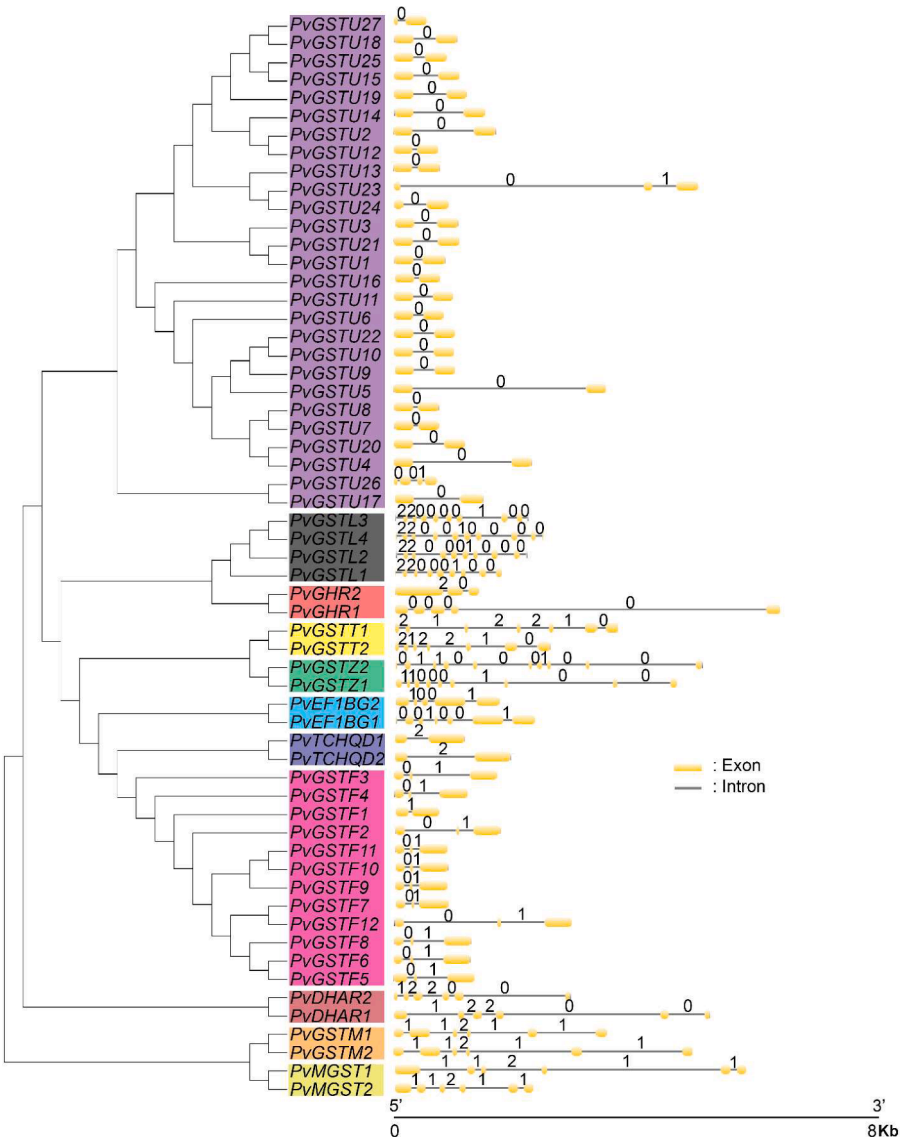

Fig. 2. The schematic diagram plotted the structure of the 59 *PvGST* genes. The clustering dendrogram was created based on the *PvGST* gene sequences. The relative length of the exon, intron, and full transcript is proportionally provided at the bottom in kilobase (Kb) scale. Numbers shown on the structure of each gene indicate the intron phases. 0, intron located between two consecutive codons; 1, intron located between the 1st and 2nd nucleotides of a codon; 2, intron located between the 2nd and 3rd nucleotides of a codon.

Additionally, we examined the syntenic association between *PvGST* genes and other bean species as well as model plants (Figure S4). No syntenic *GST* pair was identified between common bean and rice, whereas a total of 16 syntenic *GST* gene pairs were identified between common bean and *Arabidopsis* (Figure S4 and Table S6). On the other hand, a total of 41 syntenic *GST* gene pairs were found between the common bean and soybean, 26 between the common bean and barrel clover, 24 between the common bean and chickpea, and 23 between the common bean and mung bean (Figure S4 and Table S6).

Identification of the CREs in the promoter regions of the PvGST genes

In order to investigate the responsiveness of the *PvGST* genes to different stimuli, an analysis was conducted on a 2 Kb region upstream of the start codon to identify the CREs. This investigation primarily concentrated on the unique CREs associated with plant stress responses and phytohormone signaling. A total of five stress-responsive CREs, including MYB-binding site (MBS), dehydration-responsive element (DRE), MYC-binding site (MYCR), low temperature-responsive element (LTRE), and TC-rich repeats, were identified within the 46 out of the 59 promoter sequences of *PvGST* genes (Table S7). Among these five stress-responsive CREs, MBS and MYCR were mostly found in the promoter regions of the *PvGST* genes (Table S7). These findings suggested that those *PvGST* genes that contain stress-responsive CRE(s) in their promoter region might be involved in plant response to drought stress.

We next predicted the phytohormone-responsive CREs in the promoter regions of the *PvGST* genes. As expected, various types of hormone-responsive CREs, including abscisic acid (ABA)-responsive element (ABRE), ethylene-responsive element (ERE), CREs related to gibberellin responsiveness (GARE-motif and P-box), CREs related to auxin responsiveness (TGA-element and AuxRR-core), CREs related to salicylic acid responsiveness (TCA-element), and CREs related to jasmonic acid responsiveness (TGACG-motif and CGTCA-motif), were found in the promoter regions of 47 out of 59 *PvGST* genes (Table S7). More specifically, 34 and 35 *PvGST* genes contained ABRE and ERE, respectively, while 18 *PvGSTs* harbored one or both of the two gibberellin-responsive CREs in their promoter regions (Table S7). Additionally, the promoter regions of 16 *PvGST* genes contained one or

both of the two auxin-responsive CREs. Finally, 24 *PvGST* genes possessed the salicylic acid-responsive CRE, while 51 *PvGST*s harbored one or both of the two jasmonic acid-responsive CREs in their promoter region (Table S7). Taken together, the *PvGST* genes containing hormone-responsive CRE(s) might participate in pathways associated with hormones in common bean.

Expression analysis of the PvGST genes in various organs at different developmental stages and under drought and salinity

To explore the potential functions of *PvGST* genes in the growth and development of *P. vulgaris*, an examination of the expression patterns of all identified *PvGST*s was conducted across six organs at various developmental stages using publicly available RNA-sequencing datasets. Among the different *PvGST* genes, *PvGSTU2, PvGSTU15, PvGSTF1, PvGSTF5, PvGSTF9, PvGSTF10, PvGSTF11, PvEF1BG1, PvEF1BG2, PvDHAR1, PvDHAR2, PvGSTL2*, and *PvGSTL3* exhibited high expression levels in all examined organs and throughout various developmental stages (Fig. 3A; cluster II). *PvGSTU1, PvGSTU5, PvGSTU6, PvGSTU9, PvGSTU10, PvGSTU11*, and *PvGSTU22* exhibited root-specific expression patterns, while *PvGSTL1* showed specificity for both roots and seeds [seed (7 mg)] (Fig. 3A; cluster I). *PvGSTF3* exhibited specific expression in flowers (cluster I), while *PvGSTF2* showed specifically high expression in stems and flowers (cluster III) compared with their respective expression patterns in other organs (Fig. 3A). It was observed that *PvGSTU3* exhibited a considerably higher expression level in seeds, *PvGSTU17* showed elevated expression in root tips and roots, while *PvGSTU8* and *PvGSTU13* exhibited elevated expression levels in stems, shoots, and roots compared with their respective expression levels in other organs (Fig. 3A; cluster III). An intriguing observation is that the

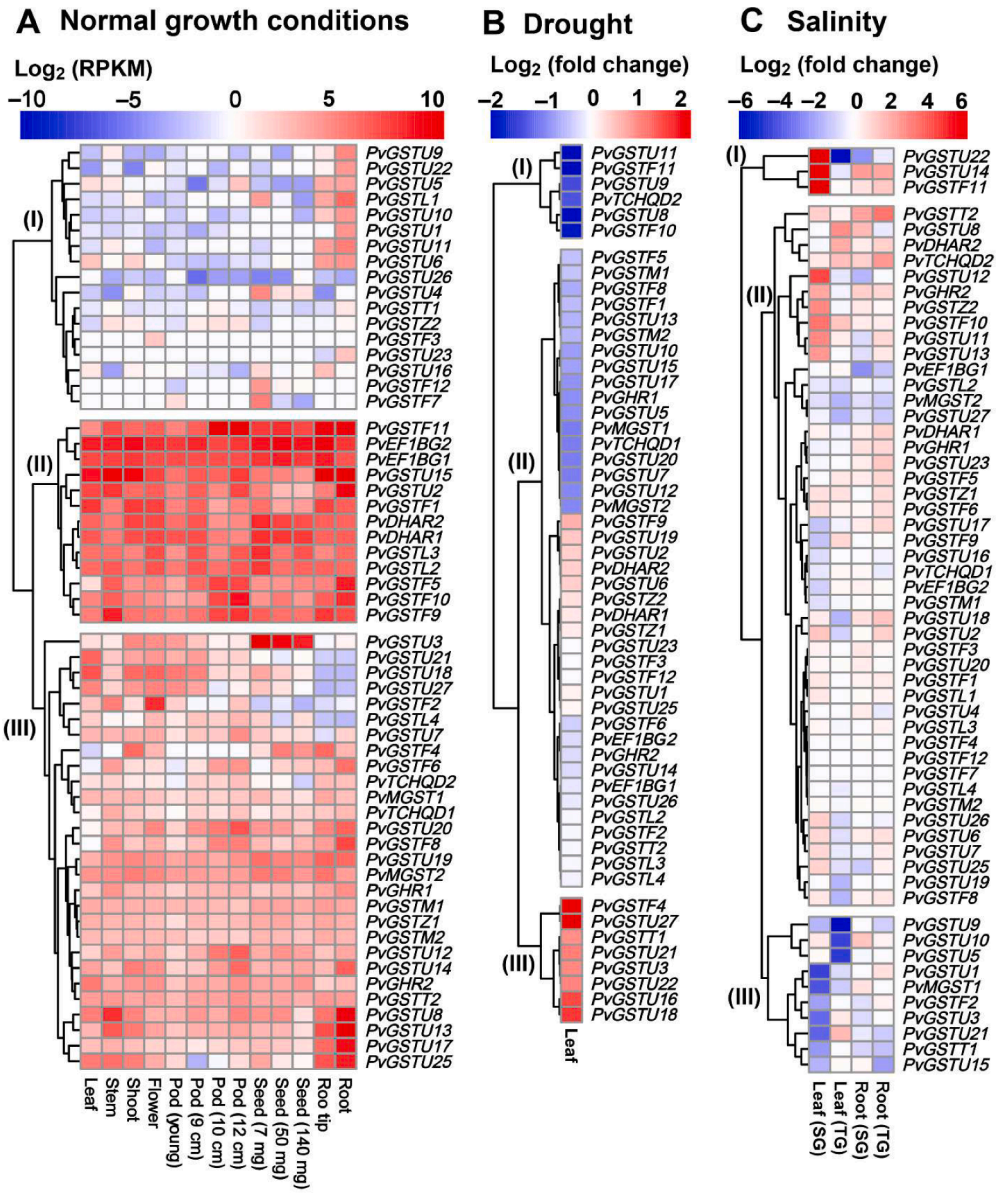

Fig. 3. Expression profiles of *PvGST* genes in various organs of common bean plants at various developmental stages and under drought or salinity. Publicly available RNA-sequencing data were used to analyze the expression levels or changes of *PvGST* genes in investigated organs and conditions. (**A**) The expression levels [$\log_2$ (RPKM)] of 59 *PvGST* genes in six organs at various developmental stages. (**B**) The expression changes [$\log_2$ (fold changes)] of 55 *PvGST* genes in leaves of common bean plants subjected to drought for 14 days at V4 stage. (**C**) The expression changes [$\log_2$ (fold changes)] of 58 *PvGST* genes in roots and leaves of susceptible (SG) and tolerant (TG) common bean genotypes subjected to gradual salinity (50, 100, and 150 mM NaCl) for five days at early seedling stage. The *PvGST* genes were divided into separate clusters depending on their expression levels or changes. The expression patterns or changes are indicated by intensities of the colors with saturation at −10 and 10 (**A**), −2 and 2 (**B**), and −6 and 6 (**C**). RPKM, reads per kilobase of transcript per million mapped reads.

expression levels of the majority of the *PvGST*s were relatively higher in roots than other organs.

To gain an insight into the potential role of *PvGST* genes in common bean responses to drought and salinity, the expression changes of 59 *PvGST*s were first analyzed using publicly available transcriptome data. Under drought, no expression data were found for *PvGSTU4, PvGSTU24, PvGSTL1*, and *PvGSTF7* genes (Fig. 3B). Among the down-regulated genes, *PvGSTU8, PvGSTU9, PvGSTU11, PvGSTF10, PvGSTF11*, and *PvTCHQD2* were the most highly down-regulated genes in common bean leaves under drought at V4 stage (Fig. 3B; cluster I). On the other hand, *PvGSTU3, PvGSTU16, PvGATU18, PvGATU21, PvGATU22, PvGATU27, PvGSTT1*, and *PvGSTF4* were the most highly up-regulated genes in leaves by drought (Fig. 3B; cluster III).

Under salinity, the expression of two contrasting genotypes (SG, susceptible genotype; TG, tolerant genotype) were assayed in the roots and leaves of common bean at early seedling stage. No expression data was found for *PvGSTU24*. A number of genes, such as *PvGSTU14* and *PvGSTT2*, showed up-regulation in roots of both SG and TG by salinity (Fig. 3C; clusters I and II). In the roots, no notable differences in the expression change patterns of the *PvGST* genes were observed between the two genotypes, except for the *PvGSTU8* that showed a higher up-regulation level by salinity in SG roots than TG roots (Fig. 3C; cluster II). As for the leaves, the *PvGST* genes displayed more variable expression change patterns in the SG than TG under salinity. Genes like *PvGSTU11, PvGSTU12, PvGSTU13, PvGSTU14, PvGSTU22, PvGSTZ2, PvGHR2, PvGSTF10*, and *PvGSTF11* showed higher up-regulation patterns (cluster I and II), while *PvGSTU1, PvGSTU3, PvGSTU15, PvGSTU21, PvGSTT1, PvMGST1*, and *PvGSTF2* showed higher down-regulation patterns (cluster III) in the SG leaves than TG leaves by salinity (Fig. 3C). Interestingly, *PvGSTU22* was highly up-regulated in SG leaves but highly down-regulated in TG leaves (Fig. 3C; cluster I), while the opposite phenomenon was observed for *PvGSTU21* under salinity (Fig. 3C; cluster III).

Effect of drought and salinity on P. vulgaris plants and stress-responsive alteration of GST enzyme activities

Drought and salinity brought noticeable negative changes to the phenotypic appearance of *P. vulgaris* plants. Wilting of the plants, yellowing, and drying of the leaves were observed in both stress conditions and the symptoms gradually increased with the increment of stress period (Fig. 4A-D). Consistent with these observations, leaf RWCs decreased significantly in responses to drought and salinity treatments (Fig. 4E). Furthermore, as the stress prolonged, the RWCs more highly dropped. A significantly higher accumulation of ROS like H_2O_2 was evident under both drought and salinity conditions (Fig. 5A, B).

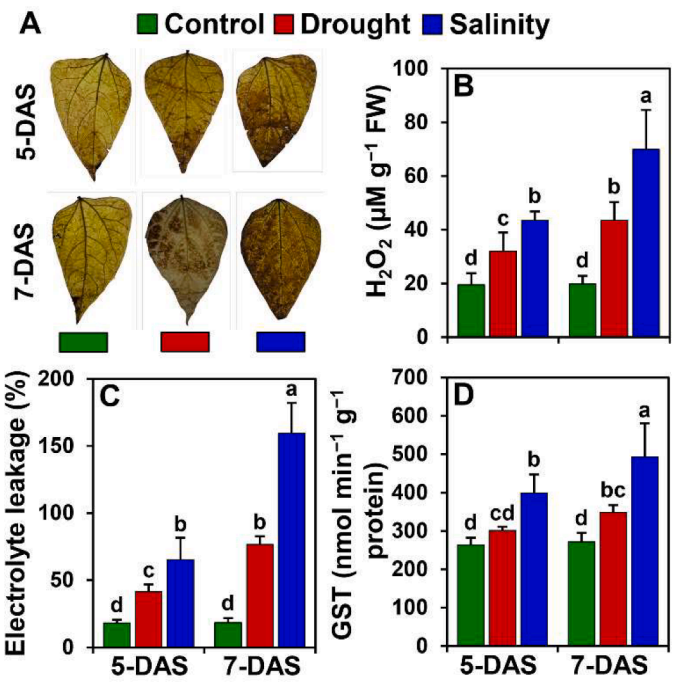

Fig. 5. Effects of drought and salinity on the oxidative stress-related markers and the activities of glutathione *S*-transferase (GST) in the leaves of common bean plants. Plants were subjected to water withholding-induced drought and 200 mM-NaCl-induced salinity treatments for five and seven days. (**A**) Diaminobenzidine (DAB)-staining for visual detection of hydrogen peroxide (H_2O_2). (**B**) H_2O_2 contents, (**C**) electrolyte leakage percentages, and (**D**) GST activities in the leaves of common bean plants after exposure to drought and salinity. Data shown are means and standard deviations ($n = 5$). Significant changes ($p < 0.05$) among the treatments are denoted by different letters above the bars, calculated using the least significant difference test. DAS, days after stress; FW, fresh weight.

Likewise, significantly higher EL percentages were noticed in both drought- and salinity-exposed plants (Fig. 5C). Additionally, under our experimental conditions, salinity level at 200 mM showed more negative impact on the physiological and biochemical responses of common bean plants than drought triggered by water-withholding treatment (Figs. 4A-E and 5A-C). Nonetheless, with the increment of the stress length, a strong induction of the GST enzyme activity was evident in stressed plants, particularly under salinity (Fig. 5D).

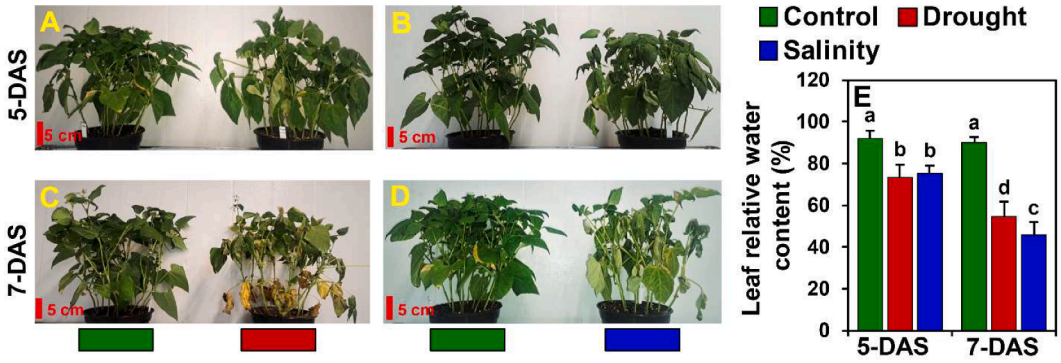

Fig. 4. Effects of drought and salinity on the phenotype of common bean plants. All pictures were taken after the plants were subjected to water withholding-induced drought and 200 mM NaCl-induced salinity treatments for five and seven days. (**A, B**) Plants subjected to drought (**A**) and salinity (**B**) for five days. (**C, D**) Plants subjected to drought (**A**) and salinity (**B**) for seven days. (**E**) Relative water contents of common bean leaves after exposure to drought or salinity. Data shown are means and standard deviations ($n = 5$). Significant changes ($p < 0.05$) among the treatments are denoted by different letters above the bars, calculated using the least significant difference test. DAS, days after stress.

Expression analysis of stress-responsive PvGST candidate genes under drought and salinity using RT-qPCR

Four genes (*PvGSTU3, PvGSTU16, PvGSTF4*, and *PvGSTT1*) up-regulated by drought (Fig. 3B; cluster III) and five (*PvGSTU11, PvGSTU12, PvGSTU13, PvGSTU14*, and *PvGSTZ2*) genes up-regulated by salinity (in the SG) in the leaves of common bean plants as shown by the RNA-sequencing data (Fig. 3C; cluster II and III) were selected for examining their expression changes in leaves of common bean under drought and salinity under our experimental conditions using RT-qPCR. Under drought, except *PvGSTU11*, all remaining genes were up-regulated, while under salinity, except *PvGSTF4*, all other genes were up-regulated at least at one time point (Fig. 6A-I). More specifically, *PvGSTU3, PvGSTU12, PvGSTU16*, and *PvGSTZ2* showed up-regulated expression patterns by drought and salinity at both time points (Fig. 6A, C, F, I), while *PvGSTU13, PvGSTU14*, and *PvGSTT1* genes displayed up-regulated expression levels by drought and salinity at least at one time point (Fig. 6D, E, H). These genes may play a role in plant responses to both drought and salinity. We also detected several genes that were responsive to either drought or salinity. Specifically, *PvGSTU11* (by 10.75- and 37.27-fold) was highly up-regulated only by salinity treatment (Fig. 6B), while *PvGSTF4* (by 76.46- and 12.21-fold, respectively) was highly up-regulated only by drought at both five and seven days of treatment (Fig. 6G). These data suggested the specific roles of these genes in plant response to salinity or drought.

Discussion

Common bean holds significant importance as a legume in both human dietary consumption and the world economy (Alcázar-Valle et al., 2020). In recent years, a great deal of effort has been given to decipher the stress signaling and adaptation processes of common bean through the identification of key regulatory genes (Shi et al., 2021; Valdisser et al., 2020; Zhang et al., 2022b, 2022a). GSTs are a group of versatile antioxidant enzymes that are widely distributed and have diverse functions in several aspects of plant physiology, development,

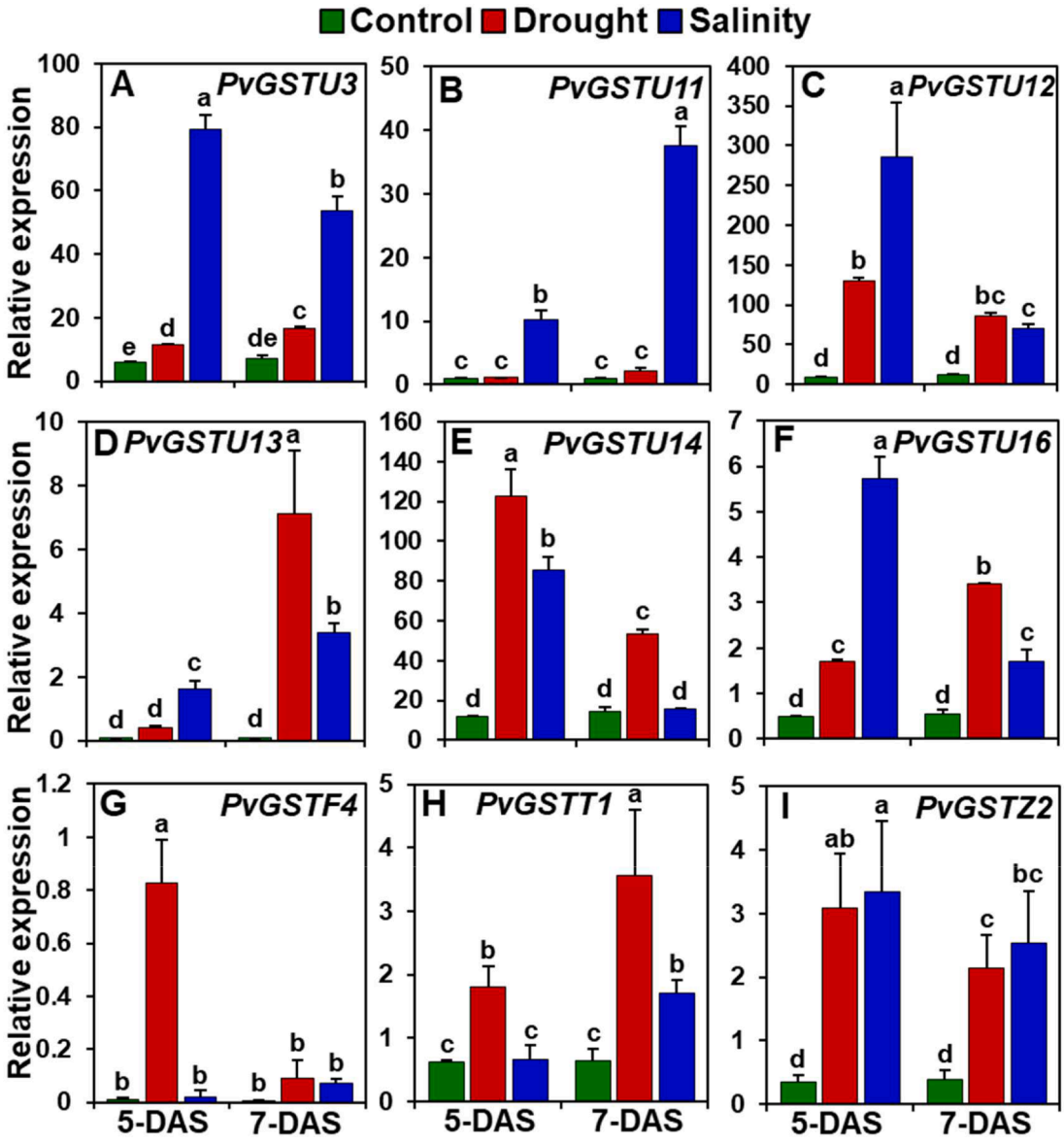

Fig. 6. Expression profiles of nine selected *PvGST* genes under drought and salinity. Expression levels of the nine *PvGST* genes were analyzed in the leaves of common bean plants in responses to the drought and salinity. Plants used for the analysis were subjected to water withholding-induced drought and 200 mM NaCl-induced salinity treatments for five and seven days. (**A-K**) Expression levels of the *PvGST* genes with standard deviations ($n = 3$). Significant changes ($p < 0.05$) among the treatments are denoted by different letters above the bars, calculated using the least significant difference test. DAS, days after stress.

and cellular defense against environmental stressors (Estévez and Hernández, 2020).

In the current study, 59 *PvGST* genes, each with at least one conserved GST-related domain (Figure S1), have been identified using extensive *in silico* genome-wide analyses. The number of identified *PvGST* genes was higher compared with 42 *GST* genes in *Zea mays* (McGonigle et al., 2000), 55 genes in *A. thaliana* (Sappl et al., 2009), 44 genes in *V. radiata* (Vaish et al., 2018), and 51 genes in *C. arietinum* (Ghangal et al., 2020), but lower compared with 79 genes in *O. sativa* (Jain et al., 2010), 74 genes in *G. max* (Ahmad et al., 2020), and 120 genes in *M. truncatula* (Hasan et al., 2021). The identified 59 PvGSTs were divided into 11 distinct classes, of which the tau class was the most abundant followed by the phi and lambda classes. Other plant species have similar distribution patterns (Figure S3); and thus, the tau, phi, and lambda class GSTs are classified as plant-specific GSTs (Ahmad et al., 2020; Hasan et al., 2021; Sappl et al., 2009). Interestingly, two metaxin class GSTs were identified in *P. vulgaris*, and this class of GSTs was only previously reported in *M. truncatula* among the studied legumes (Hasan et al., 2021). However, we did not find any hemerythrin class GSTs in *P. vulgaris*, although they were previously reported in *M. truncatula*. Duplicated genes are essential in the evolutionary process as it is required for the emergence of novel biological functions and the extension of gene families (Xu et al., 2020). Analysis of gene duplication events revealed that both segmental and tandem duplications played a role in the expansion of the *PvGST* family (Fig. 1). Additionally, the Ka/Ks ratio was employed to examine the selection pressures acting on duplicated genes. When the Ka/Ks ratio is more than one, it indicates positive selection. A Ka/Ks ratio of one suggests neutral selection, while a ratio below one indicates negative or purifying selection (Islam et al., 2017). The Ka/Ks ratios of all duplicated *PvGST*s (except for *PvGHR1/PvGHR2, PvDHAR1/PvDHAR2*, and *PvGSTU23/PvGSTU24*) were smaller than 1 (Table S4), indicating the presence of purifying selection in the evolutionary process of these gene pairs.

In vitro stability of a protein can be predicted through its II. If a protein has II score below 40, it is predicted to be stable under *in vitro* conditions (Gamage et al., 2019). A total of 23 out of 59 PvGSTs had II below 40 (Table S3), suggesting their high stability under *in vitro* conditions. On the other hand, the AI quantifies the spatial occupancy in the volume by the aliphatic side chains of the amino acids alanine, isoleucine, leucine, and valine (Hoda et al., 2021). AI also measures the thermostability of a given protein. A protein is considered thermostable if the AI value is greater than 71 (Hoda et al., 2021). All the 59 PvGST proteins identified in the current study had an AI value higher than 71 (Table S3), suggesting their functionality in a wide range of temperature regime. Nonetheless, based on pI values, 12 out of 59 PvGST proteins were basic (pI $>$ 7), while 47 were acidic (pI $<$ 7). There is a direct correlation between the pI of a protein and its subcellular localization. The proteins acidic in nature tend to localize in cytoplasm, while the proteins basic in nature localize in mitochondria and nucleus (Tokmakov et al., 2021). This observation supports our findings as the PvGST proteins identified as acidic were mostly found to be localized in cytoplasm, while those PvGSTs identified as basic mostly localized in mitochondria and nucleus (Table S3). Apart from cytoplasm and mitochondria, some of the PvGST proteins were also predicted to localize in chloroplasts, endoplasmic reticulum, and extracellular matrix (Table S3). The wide range of subcellular distribution might suggest the wide range of functionality of the PvGST proteins. Except for PvDHAR2, all other PvGST proteins had a negative GRAVY value, suggesting that they are polar hydrophilic in nature (Bhattacharya et al., 2018).

Gene structure analysis revealed that intron/exon number, position, and phase were homogeneous within the same class *PvGST*s, and each class showed substantial differences in gene structure compared with the other classes (Fig. 2). The presence of structural heterozygosity may suggest that these gene classes had gone through divergent evolutionary trajectories. The conservation of splicing sites is closely linked to the intron phase and is believed to be connected to the evolutionary development of the spliceosome machinery (Poverennaya and Roytberg, 2020). The level of conservation is highest in intron phase 0, whereas intron phase 2 exhibits the lowest conservation (Islam et al., 2017). Intron phase 1, on the other hand, has an intermediate level of conservation (Islam et al., 2017). The members of the tau class PvGST proteins exhibited the greatest degree of conservation as they were associated with intron phase 0, whereas the TCHQD class had the lowest level of conservation as they were associated with intron phase 2 (Fig. 2). The remaining classes exhibited higher intron counts, accompanied by a combination of conserved and non-conserved splicing site sequences (Fig. 2).

The N-terminal domain of GSTs is the center of their catalytic activity (Islam et al., 2017), and 54 out of the 59 PvGST proteins found to contain N-terminal GST domain (Figure S1). On the other hand, the results of the motif analysis revealed that motif 1, which represents the N-terminal domain, was conserved across majority of the PvGST proteins (Figure S2 and Table S5). Most of the other motifs exhibited class selectivity, which might suggest that they possess distinct functions that are limited to the corresponding protein classes.

Phylogenetic analysis of 442 GST proteins derived from *P. vulgaris, A. thaliana, M. truncatula, C. arietinum, V. radiata, O. sativa*, and *G. max* suggested high levels of similarity among different classes of GST proteins. All the GST proteins strictly follow the domain-based classification and were grouped into 12 monophyletic groups (Figure S3). This observation might suggest that the evolutionary and divergent processes of each GST class occurred prior to the divergence of monocotyledonous and dicotyledonous plants (Islam et al., 2017). The pattern of GST members distribution across different classes consistent with previous research (Islam et al., 2019; Wang et al., 2019). Nevertheless, synteny analysis suggested that the *PvGST* members exhibited a closer genetic relationship with *G. max, M. truncatula, V. radiata*, and *C. arietinum* in contrast with their counterparts in *A. thaliana* and *O. sativa* (Figure S4). This finding might suggest the fact that legumes, being part of the eudicot superfamily, were diverged more recently from a common ancestral lineage.

Gene expression analysis of *PvGST*s provided an insight into their function in plant physiology and development. Organ- and developmental stage-specific expression patterns were observed for most of the *PvGST*s. In addition, 13 genes were found to maintain ubiquitous constitutive expression patterns in examined organs and across developmental stages (Fig. 3A; cluster II). About half of the *PvGST*s showed root-specific expression, suggesting their important function in the roots. Interestingly, most of the tandemly duplicated and some of the segmentally duplicated gene pairs exhibited variable expression patterns under normal and stress conditions (Figs. 1, 3), which might imply that the retention of gene duplicates in responses to stresses might be associated with the processes of gene expression divergence (Huerta-cepas et al., 2011), and these gene pairs might have specific functions in certain organs during drought and/or salinity. For instance, *PvGSTT1* had a low expression level under control conditions in almost all examined organs and across investigated developmental stages (Fig. 3A; cluster I), while its expression was up-regulated in the leaves under drought (Fig. 3B; cluster III). On the other hand, its partner *PvGSTT2* in the tandemly duplicated pair showed constitutive and ubiquitous expression patterns in all examined organs and across investigated developmental stages under normal conditions, while its expression was up-regulated under salt stress in the roots and leaves of both SG and TG (Fig. 3A; cluster III and C; cluster II). It is plausible to suggest that *PvGSTT1* and *PvGSTT2* might have played an important defensive function in *P. vulgaris* under water-deficit and salinity conditions, respectively. Nonetheless, the RT-qPCR data revealed that out of nine tested genes, *PvGSTU3, PvGSTU12, PvGSTU13, PvGSTU14, PvGSTU16, PvGSTT1*, and *PvGSTZ2*, exhibited the up-regulation in responses to both drought and salt conditions (Fig. 6A, C-F, H, I). On the other hand, *PvGSTU11* was up-regulated only by salinity, while *PvGSTF4* was only by drought (Fig. 6B, G). Interestingly, all these nine stress-inducible

genes were enriched with at least one drought-responsive MBS and/or MYCR *cis*-regulatory elements (Table S7). Additionally, *PvGSTU3, PvGSTU13, PvGSTU14*, and *PvGSTF4* were enriched with LTRE (Table S7). The presence of multiple stress-responsive *cis*- regulatory elements might suggest their important role in mitigation of multiple stresses in plants. Nonetheless, apart from stress-responsive CREs, the promoter regions of all the above-mentioned stress-inducible genes were enriched with at least one type of phytohormone-responsive CREs (Table S7). It is well recognized that many plant hormones have a role in controlling stress responses (Gupta et al., 2020). Such enrichment with hormone-responsive CREs in their promoter regions suggests that related hormones may play an important role in modulating the expression of the above-mentioned genes. Nevertheless, the RT-qPCR results were partially in agreement with the RNA-sequencing data that revealed the up-regulation of *PvGSTU3, PvGSTU16, PvGSTF4*, and *PvGSTT1* in the leaves of common bean plants at the V4 stage only by drought (Fig. 3B; cluster III) (Gregorio Jorge et al., 2020), and the up-regulation of *PvGSTU11, PvGSTU12, PvGSTU13, PvGSTU14*, and *PvGSTZ2* in leaves of the susceptible 14-day-old common bean seedlings only by salinity (Fig. 3C; cluster III) (Niron et al., 2020). However, the RT-qPCR data shown in Fig. 6 revealed several genes, such as *PvGSTU3, PvGSTU12, PvGSTU13, PvGSTU14, PvGSTU16, PvGSTT1*, and *PvGSTZ2*, were up-regulated in common bean leaves by both drought and salinity as discussed above. The possible reason for the observed disparity among the RT-qPCR and RNA-sequencing results might be attributed to the utilization of a single timepoint in the RNA-sequencing and/or the variations in development stages and stress treatment conditions. Furthermore, genotype difference might also be a contributing factor to the observed disparity. Indeed, genotype-specific salinity-responsive expression patterns of *PvGST*s in the leaves of *P. vulgaris* were observed in RNA-sequencing data, with SG showing a more up-regulating expression trend of *PvGST*s than TG under salinity (Fig. 3C) (Niron et al., 2020).

There is a widely accepted belief that the formation of stress-induced ROS is associated with oxidative damage and hinders the development of plants (Bano et al., 2021). This association has been clearly shown in common bean plants that were subjected to drought and salt stress (Figs. 4A-D and 5A-C). Plants under drought and salt stress exhibited elevated levels of H_2O_2, leading to an increased membrane damage as evident by higher degree of EL (Fig. 5A-C). Additionally, it was found that the overall activity of GST enzymes dramatically increased in the presence of drought or salt stressor (Fig. 5D), suggesting its potential correlation with the heightened buildup of ROS. The increased activity of GST in common bean plants in response to drought and salt stress might trigger the activation of the GST-dependent peroxide detoxification mechanism, which serves to boost the plants defense against oxidative damage caused by drought and salinity (Estévez and Hernández, 2020). Importantly, the up-regulated expression of many *PvGST* genes may contribute to the concurrent elevation of their respective enzyme activity. Collectively, our findings offer a thorough examination of the *GST* gene family in *P. vulgaris* and solidify the role of the GSTs as prominent stress biomarkers in plants.

Funding

This research did not receive any specific grant from funding agencies in the public, commercial, or not-for-profit sectors.

CRediT authorship contribution statement

Touhidur Rahman Anik: Conceptualization, Data curation, Formal analysis, Methodology, Software, Validation, Writing – original draft. **Ha Duc Chu:** Data curation, Formal analysis, Methodology, Software, Validation, Writing – review & editing. **Md. Shahabuddin Ahmed:** Formal analysis, Methodology, Software. **Chien Van Ha:** Methodology, Supervision. **Sunil S. Gangurde:** Resources, Writing – review & editing. **Md. Arifur Rahman Khan:** Visualization, Writing – review & editing. **Thao Duc Le:** Visualization, Writing – review & editing. **Dung Tien Le:** Visualization, Writing – review & editing. **Mostafa Abdelrahman:** Formal analysis, Validation, Writing – review & editing. **Lam-Son Phan Tran:** Conceptualization, Methodology, Project administration, Resources, Supervision, Validation, Writing – review & editing.

Declaration of competing interest

The authors declare that they have no known competing financial interests or personal relationships that could have appeared to influence the work reported in this paper.

Data availability

All data are available in the manuscript.

Acknowledgment

The authors have not received any form of assistance to disclose.

Supplementary materials

Supplementary material associated with this article can be found, in the online version, at doi:10.1016/j.stress.2024.100489.

References

Ahmad, M.Z., Nasir, J.A., Ahmed, S., Ahmad, B., Sana, A., Salman, S., Shah, Z., Yang, C. Y., 2020. Genome-wide analysis of glutathione *S*-transferase gene family in *G. max*. Biologia (Bratisl) 75, 1691–1705.

Alcázar-Valle, M., Lugo-Cervantes, E., Mojica, L., Morales-Hernández, N., Reyes-Ramírez, H., Enríquez-Vara, J.N., García-Morales, S., 2020. Bioactive compounds, antioxidant activity, and antinutritional content of legumes: a comparison between four *Phaseolus* species. Molecules 25, 3528.

Arteaga, S., Yabor, L., Díez, M.J., Prohens, J., Boscaiu, M., Vicente, O., 2020. The use of proline in screening for tolerance to drought and salinity in common bean (*Phaseolus vulgaris* L.) genotypes. Agronomy 10, 817.

Bailey, T.L., Johnson, J., Grant, C.E., Noble, W.S., 2015. The MEME suite. Nucl. Acids Res. 43, W39–W49.

Bano, A., Gupta, A., Rai, S., Fatima, T., Sharma, S., Pathak, N., 2021. Mechanistic role of reactive oxygen species and its regulation via the antioxidant system under environmental stress. *Plant stress physiology—perspectives in agriculture*. IntechOpen, 1–18.

Bhattacharya, M., Hota, A., Kar, A., Sankar Chini, D., Chandra Malick, Chandra Patra, B., Kumar Das, B., 2018. *In silico* structural and functional modelling of Antifreeze protein (AFP) sequences of Ocean pout (*Zoarces americanus*, Bloch & Schneider 1801). J. Genet. Eng. Biotechnol. 16, 721–730.

Borges, A., Tsai, S.M., Caldas, D.G.G., 2012. Validation of reference genes for RT-qPCR normalization in common bean during biotic and abiotic stresses. Plant Cell Rep. 31, 827–838.

Burbano-Erazo, E., León-Pacheco, R.I., Cordero-Cordero, C.C., López-Hernández, F., Cortés, A.J., Tofiño-Rivera, A.P., 2021. Multi-environment yield components in advanced common bean (*Phaseolus vulgaris* l.) × tepary bean (*P. acutifolius* a. gray) interspecific lines for heat and drought tolerance. Agronomy 11, 1978.

Chen, C., Chen, H., Zhang, Y., Thomas, H.R., Frank, M.H., He, Y., Xia, R., 2020. TBtools: an integrative toolkit developed for interactive analyses of big biological data. Mol. Plant 13, 1194–1202.

Contreras-Moreira, B., Naamati, G., Rosello, M., Allen, J.E., Hunt, S.E., Muffato, M., Gall, A., Flicek, P., 2022. Scripting analyses of genomes in ensembl plants. Methods Mol. Biol. 2443, 27–55.

Dixon, D.P., Lapthorn, A., Edwards, R., 2002. Plant glutathione transferases. Genome Biol. 3, 1–10.

Dong, Y., Li, C., Zhang, Y., He, Q., Daud, M.K., Chen, J., Zhu, S., 2016. Glutathione *S*-transferase gene family in *Gossypium raimondii* and *G. arboreum*: comparative genomic study and their expression under salt stress. Front. Plant Sci. 7, 181059.

Emamverdian, A., Ding, Y., Hasanuzzaman, M., Barker, J., Liu, G., Li, Y., Mokhberdoran, F., 2023. Insight into the biochemical and physiological mechanisms of nanoparticles-induced arsenic tolerance in bamboo. Front. Plant Sci. 14, 1121886.

Estévez, I.H., Hernández, M.R., 2020. Plant glutathione *S*-transferases: an overview. Plant Gene 23, 100233.

Fang, X., An, Y., Zheng, J., Shangguan, L., Wang, L., 2020. Genome-wide identification and comparative analysis of *GST* gene family in apple (*Malus domestica*) and their expressions under ALA treatment. Biotech 3 10,, 1–16.

Gamage, D.G., Gunaratne, A., Periyannan, G.R., Russell, T.G., 2019. Applicability of instability index for *In vitro* protein stability prediction. Protein Pept. Lett. 26, 339–347.
Gasteiger, E., Hoogland, C., Gattiker, A., Duvaud, S.E., Wilkins, M.R., Appel, R.D., Bairoch, A., 2005. *Protein identification and analysis tools on the ExPASy server*. Humana press, pp. 571–607.
Ghangal, R., Rajkumar, M.S., Garg, R., Jain, M., 2020. Genome-wide analysis of glutathione S-transferase gene family in chickpea suggests its role during seed development and abiotic stress. Mol. Biol. Rep. 47, 2749–2761.
Gregorio Jorge, J., Villalobos-López, M.A., Chavarría-Alvarado, K.L., Ríos-Meléndez, S., López-Meyer, M., Arroyo-Becerra, A., 2020. Genome-wide transcriptional changes triggered by water deficit on a drought-tolerant common bean cultivar. BMC Plant Biol. 20, 1–20.
Gupta, A., Sinha, R., Fernandes, J.L., Abdelrahman, M., Burritt, D.J., Tran, L.S.P., 2020. Phytohormones regulate convergent and divergent responses between individual and combined drought and pathogen infection. Crit. Rev. Biotechnol. 40, 320–340.
Han, X.M., Yang, Z.L., Liu, Y.J., Yang, H.L., Zeng, Q.Y., 2018. Genome-wide profiling of expression and biochemical functions of the Medicago glutathione *S*-transferase gene family. Plant Physiol. Biochem. 126, 126–133.
Hao, Y., Xu, S., Lyu, Z., Wang, H., Kong, L., Sun, S., 2021. Comparative analysis of the glutathione *S*-transferase gene family of four *Triticeae* species and transcriptome analysis of GST genes in common wheat responding to salt stress. Int. J. Genomics 2021, 1–11.
Hasan, M.S., Islam, S., Hasan, M.N., Sajib, S.Das, Ahmed, S., Islam, T., Ghosh, A., 2020. Genome-wide analysis and transcript profiling identify several abiotic and biotic stress-responsive Glutathione *S*-transferase genes in soybean. Plant Gene 23, 100239.
Hasan, M.S., Singh, V., Islam, S., Islam, M.S., Ahsan, R., Kaundal, A., Islam, T., Ghosh, A., 2021. Genome-wide identification and expression profiling of glutathione *S*-transferase family under multiple abiotic and biotic stresses in *Medicago truncatula* L. PLoS ONE 16, e0247170.
Hoda, A., Tafaj, M., Sallaku, E., 2021. *In silico* structural, functional and phylogenetic analyses of cellulase from *Ruminococcus albus*. J. Genet. Eng. Biotechnol. 19, 58.
Huerta-cepas, J., Dopazo, J., Huynen, M.A., Gabaldón, T., 2011. Evidence for short-time divergence and long-time conservation of tissue-specific expression after gene duplication. Brief Bioinform. 12, 442–448.
Islam, M.A., Rahman, Md Mustafizur, Rahman, Md Mizanor, Jin, X., Sun, L., Zhao, K., Wang, S., Sikdar, A., Noor, H., Jeon, J.S., Zhang, W., Sun, D., 2021. *In silico* and transcription analysis of trehalose-6-phosphate phosphatase gene family of wheat: trehalose synthesis genes contribute to salinity, drought stress and leaf senescence. Genes (Basel) 12, 1652.
Islam, S., Rahman, I.A., Islam, T., Ghosh, A., 2017. Genome-wide identification and expression analysis of glutathione *S*-transferase gene family in tomato: gaining an insight to their physiological and stress-specific roles. PLoS ONE 12, e0187504.
Islam, S., Sajib, S.D., Jui, Z.S., Arabia, S., Islam, T., Ghosh, A., 2019. Genome-wide identification of glutathione *S*-transferase gene family in pepper, its classification, and expression profiling under different anatomical and environmental conditions. Sci. Rep. 9, 9101.
Jain, M., Ghanashyam, C., Bhattacharjee, A., 2010. Comprehensive expression analysis suggests overlapping and specific roles of rice glutathione *S*-transferase genes during development and stress responses. BMC Genomics 11, 1–17.
Kim, Y.S., Park, S.I., Kim, J.J., Shin, S.Y., Kwak, S.S., Lee, C.H., Park, H.M., Kim, Y.H., Kim, I.S., Yoon, H.S., 2022. Over-expression of dehydroascorbate reductase improves salt tolerance, environmental adaptability and productivity in *Oryza sativa*. Antioxidants 11, 1077.
Kuluev, B.R., Ermoshin, A.A., Mikhaylova, E.V., 2022. Overexpression of the glutathione *S*-transferase *ATGSTF11* gene improves growth and abiotic stress tolerance of tobacco transgenic plants. Russian J. Plant Physiol. 69, 148.
Kumar, S., Asif, M.H., Chakrabarty, D., Tripathi, R.D., Dubey, R.S., Trivedi, P.K., 2013. Expression of a rice Lambda class of glutathione *S*-transferase, *OsGSTL2*, in *Arabidopsis* provides tolerance to heavy metal and other abiotic stresses. J. Hazard Mater. 248, 228–237.
Kumar, S., Trivedi, P.K., 2018. Glutathione *S*-transferases: role in combating abiotic stresses including arsenic detoxification in plants. Front. Plant Sci. 9, 364396.
Kwak, M., Gepts, P., 2009. Structure of genetic diversity in the two major gene pools of common bean (*Phaseolus vulgaris* L., Fabaceae). Theor. Appl. Genet. 118, 979–992.
Lallement, P.A., Brouwer, B., Keech, O., Hecker, A., Rouhier, N., 2014. The still mysterious roles of cysteine-containing glutathione transferases in plants. Front. Pharmacol. 5, 105046.
Lescot, M., Déhais, P., Thijs, G., Marchal, K., Moreau, Y., Van De Peer, Y., Rouzé, P., Rombauts, S., 2002. PlantCARE, a database of plant cis-acting regulatory elements and a portal to tools for *in silico* analysis of promoter sequences. Nucl. Acids Res. 30, 325–327.
Lu, S., Wang, J., Chitsaz, F., Derbyshire, M.K., Geer, R.C., Gonzales, N.R., Gwadz, M., Hurwitz, D.I., Marchler, G.H., Song, J.S., Thanki, N., Yamashita, R.A., Yang, M., Zhang, D., Zheng, C., Lanczycki, C.J., Marchler-Bauer, A., 2020. CDD/SPARCLE: the conserved domain database in 2020. Nucl. Acids Res. 48, D265–D268.
McConnell, M., Mamidi, S., Lee, R., Chikara, S., Rossi, M., Papa, R., McClean, P., 2010. Syntenic relationships among legumes revealed using a gene-based genetic linkage map of common bean (*Phaseolus vulgaris* L.). Theor. Appl. Genet. 121, 1103–1116.
McGonigle, B., Keeler, S.J., Lau, S.M.C., Koeppe, M.K., O'Keefe, D.P., 2000. A genomics approach to the comprehensive analysis of the glutathione *S*-transferase gene family in soybean and maize. Plant Physiol 124, 1105–1120.
Mistry, J., Chuguransky, S., Williams, L., Qureshi, M., Salazar, G.A., Sonnhammer, E.L.L., Tosatto, S.C.E., Paladin, L., Raj, S., Richardson, L.J., Finn, R.D., Bateman, A., 2021. Pfam: the protein families database in 2021. Nucl. Acids Res. 49, D412–D419.
Mostofa, M.G., Fujita, M., 2013. Salicylic acid alleviates copper toxicity in rice (*Oryza sativa* L.) seedlings by up-regulating antioxidative and glyoxalase systems. Ecotoxicology 22, 959–973.
Niron, H., Barlas, N., Salih, B., Türet, M., 2020. Comparative transcriptome, metabolome, and ionome analysis of two contrasting common bean genotypes in saline conditions. Front. Plant Sci. 11, 599501.
Nishiyama, R., Watanabe, Y., Fujita, Y., Le, D.T., Kojima, M., Werner, T., Vankova, R., Yamaguchi-Shinozaki, K., Shinozaki, K., Kakimoto, T., Sakakibara, H., Schmülling, T., Tran, L.S.P., 2011. Analysis of cytokinin mutants and regulation of cytokinin metabolic genes reveals important regulatory roles of cytokinins in drought, salt and abscisic acid responses, and abscisic acid biosynthesis. Plant Cell 23, 2169–2183.
O'Rourke, J.A., Iniguez, L.P., Fu, F., Bucciarelli, B., Miller, S.S., Jackson, S.A., McClean, P.E., Li, J., Dai, X., Zhao, P.X., Hernandez, G., Vance, C.P., 2014. An RNA-Seq based gene expression atlas of the common bean. BMC Genomics 15, 1–17.
Poverennaya, I.V., Roytberg, M.A., 2020. Spliceosomal introns: features, functions, and evolution. Biochemistry (Moscow) 85, 725–734.
Rezaei, M.K., Shobbar, Z.S., Shahbazi, M., Abedini, R., Zare, S., 2013. Glutathione *S*-transferase (GST) family in barley: identification of members, enzyme activity, and gene expression pattern. J. Plant Physiol. 170, 1277–1284.
Sappl, P.G., Carroll, A.J., Clifton, R., Lister, R., Whelan, J., Harvey Millar, A., Singh, K.B., 2009. The *Arabidopsis* glutathione transferase gene family displays complex stress regulation and co-silencing multiple genes results in altered metabolic sensitivity to oxidative stress. Plant J. 58, 53–68.
Schmutz, J., McClean, P.E., Mamidi, S., Wu, G.A., Cannon, S.B., Grimwood, J., Jenkins, J., Shu, S., Song, Q., Chavarro, C., Torres-Torres, M., Geffroy, V., Moghaddam, S.M., Gao, D., Abernathy, B., Barry, K., Blair, M., Brick, M.A., Chovatia, M., Gepts, P., Goodstein, D.M., Gonzales, M., Hellsten, U., Hyten, D.L., Jia, G., Kelly, J.D., Kudrna, D., Lee, R., Richard, M.M.S., Miklas, P.N., Osorno, J.M., Rodrigues, J., Thareau, V., Urrea, C.A., Wang, M., Yu, Y., Zhang, M., Wing, R.A., Cregan, P.B., Rokhsar, D.S., Jackson, S.A., 2014. A reference genome for common bean and genome-wide analysis of dual domestications. Nat. Genet. 46, 707–713.
Sharma, R., Sahoo, A., Devendran, R., Jain, M., 2014. Over-expression of a rice tau class glutathione *S*-transferase gene improves tolerance to salinity and oxidative stresses in *Arabidopsis*. PLoS ONE 9, e92900.
Shi, A., Gepts, P., Song, Q., Xiong, H., Michaels, T.E., Chen, S., 2021. Genome-wide association study and genomic prediction for soybean cyst nematode resistance in USDA common bean (*Phaseolus vulgaris*) core collection. Front. Plant Sci. 12, 624156.
Sofi, P.A., Rehman, K., Gull, M., Kumari, J., Djanaguiraman, M., Prasad, P.V.V., 2021. Integrating root architecture and physiological approaches for improving drought tolerance in common bean (*Phaseolus vulgaris* L.). Plant Physiol. Rep. 26, 4–22.
Srivastava, D., Verma, G., Chauhan, A.S., Pande, V., Chakrabarty, D., 2019. Rice (*Oryza sativa* L.) tau class glutathione *S*-transferase (*OsGSTU30*) overexpression in *Arabidopsis thaliana* modulates a regulatory network leading to heavy metal and drought stress tolerance. Metallomics 11, 375–389.
Tamura, K., Stecher, G., Kumar, S., 2021. MEGA11: molecular evolutionary genetics analysis version 11. Mol. Biol. Evol. 38, 3022–3027.
Tokmakov, A.A., Kurotani, A., Sato, K.I., 2021. Protein pI and intracellular localization. Front. Mol. Biosci. 8, 775736.
Vaish, S., Awasthi, P., Tiwari, S., Tiwari, S.K., Gupta, D., Basantani, M.K., 2018. *In silico* genome-wide identification and characterization of the glutathione *S*-transferase gene family in *Vigna radiata*. Genome 61, 311–322.
Valdisser, P.A.M.R., Müller, B.S.F., de Almeida Filho, J.E., Morais Júnior, O.P., Guimarães, C.M., Borba, T.C.O., de Souza, I.P., Zucchi, M.I., Neves, L.G., Coelho, A.S. G., Brondani, C., Vianello, R.P., 2020. Genome-wide association studies detect multiple QTLs for productivity in mesoamerican diversity panel of common bean under drought stress. Front. Plant Sci. 11, 574674.
Wagner, U., Edwards, R., Dixon, D.P., Mauch, F., 2002. Probing the diversity of the *Arabidopsis* glutathione *S*-transferase gene family. Plant Mol. Biol. 49, 515–532.
Wang, L., Fu, H., Zhao, J., Wang, J., Dong, S., Yuan, X., Li, X., Chen, M., 2023. Genome-wide identification and expression profiling of glutathione *S*-transferase gene family in foxtail millet (*Setaria italica* L.). Plants 12, 1138.
Wang, R., Ma, J., Zhang, Q., Wu, C., Zhao, H., Wu, Y., Yang, G., He, G., 2019. Genome-wide identification and expression profiling of glutathione transferase gene family under multiple stresses and hormone treatments in wheat (*Triticum aestivum* L.). BMC Genomics 20, 1–15.
Xu, J., Tian, Y.S., Xing, X.J., Peng, R.H., Zhu, B., Gao, J.J., Yao, Q.H., 2016. Over-expression of *AtGSTU19* provides tolerance to salt, drought and methyl viologen stresses in *Arabidopsis*. Physiol. Plant 156, 164–175.
Xu, J., Zheng, A.Q., Xing, X.J., Chen, L., Fu, X.Y., Peng, R.H., Tian, Y.S., Yao, Q.H., 2018. Transgenic *Arabidopsis* plants expressing grape glutathione *S*-transferase gene (*VvGSTF13*) show enhanced tolerance to abiotic stress. Biochemistry (Moscow) 83, 755–765.
Xu, Z., Xu, Z., Pu, X., Gao, R., Demurtas, O.C., Fleck, S.J., Richter, M., He, C., He, C., Ji, A., Sun, W., Kong, J., Hu, K., Ren, F., Ren, F., Song, Jiejie, Wang, Z., Gao, T., Xiong, C., Yu, H., Xin, T., Albert, V.A., Giuliano, G., Chen, S., Song, J., Song, J., Song, J., 2020. Tandem gene duplications drive divergent evolution of caffeine and crocin biosynthetic pathways in plants. BMC Biol. 18, 1–14.
Yang, Q.Q., Gan, R.Y., Ge, Y.Y., Zhang, D., Corke, H., 2018. Polyphenols in common beans (*Phaseolus vulgaris* L.): chemistry, analysis, and factors affecting composition. Compr. Rev. Food Sci. Food Saf. 17, 1518–1539.

Yu, C.S., Chen, Y.C., Lu, C.H., Hwang, J.K., 2006. Prediction of protein subcellular localization. Proteins Struct. Funct. Genet. 64, 643–651.

Zhang, Q., Geng, J., Du, Y., Zhao, Q., Zhang, W., Fang, Q., Yin, Z., Li, J., Yuan, X., Fan, Y., Cheng, X., Du, J., 2022a. Heat shock transcription factor (Hsf) gene family in common bean (*Phaseolus vulgaris*): genome-wide identification, phylogeny, evolutionary expansion and expression analyses at the sprout stage under abiotic stress. BMC Plant Biol. 22, 32.

Zhang, Q., Zhang, W.jing, Yin, Z.gong, Li, W.jia, Xia, C.Y., Sun, H.Y., Yang, Y.M., Wu, H. Bin, Zhang, S., Zhao, H.hao, Zhang, W.H., Guo, Y.xia, Du, J.D., Zhao, Q., 2022b. Genome-wide identification reveals the potential functions of the *bZIP* gene family in common bean (*Phaseolus vulgaris*) in response to salt stress during the sprouting stage. J. Plant Growth Regul. 41, 3075–3090.